Journal of Alloys and Compounds 502 (2010) 80–86

Contents lists available at ScienceDirect

Journal of Alloys and Compounds

journal homepage: www.elsevier.com/locate/jallcom

# A study of the effect of aluminum on $MoSi_2$ formation by self-propagation high-temperature synthesis

S. Hasani, M. Panjepour*, M. Shamanian

*Department of Materials Engineering, Isfahan University of Technology, 84156-83111 Isfahan, Iran*

ARTICLE INFO

*Article history:*
Received 10 January 2010
Received in revised form 13 April 2010
Accepted 23 April 2010
Available online 5 May 2010

*Keywords:*
Combustion synthesis
$MoSi_2$ formation
Self-propagation high-temperature synthesis
Aluminum
The oxidation of aluminum

ABSTRACT

In this study, the self-propagation high-temperature synthesis (SHS) for the formation of $MoSi_2$ in the presence of aluminum was investigated. Test specimens with nominal compositions including (Mo + 2Si) with stoichiometric ratio and (Mo + 2Si) + 5 wt% Al were employed. Each of the different samples was tested for SHS to determine the thermal profile and differential thermal analysis (DTA) under air atmosphere. The registered thermal profiles resulted for the two samples showed the maximum temperature increase (about 400 °C) in the combustion front in the presence of aluminum. The DTA results also showed that the area of silicon melting point on the DTA curve was deleted in the presence of aluminum. On the other hand, the X-ray diffraction (XRD), scanning electron microscope (SEM) and energy dispersive spectrometer (EDS) studies indicated that the SHS reaction between Mo and Si was done in a more complete manner in the presence of aluminum and aluminum particles were all oxidized.



## 1. Introduction

Properties of molybdenum disilicide ($MoSi_2$) such as high heat resistance, high melting point (2020 °C), high electrical conductivity, and excellent corrosion resistance at high temperatures all have resulted in an ever-expanding application range of this material in different industries [1–4]. The production of this material is done through different techniques. Of these techniques which have been of interest to many researchers, is the self-propagation high-temperature synthesis (SHS). In fact, intense heat resulting from the reaction between molybdenum and silicon provides the conditions for the production of molybdenum disilicide by this technique [5]. Many research activities have been performed on Mo–Si system SHS without or with the presence of a third element from different aspects so far. For example, in 1995, Seetharama [6] studied the penetration reactions in $MoSi_2$ by SHS process. Jo et al. [7] in 1996 studied and investigated the SHS performing mechanism in Mo–Si system. The structure of combustion wave during the production of $MoSi_2$, by stimulated (mechanically) SHS process was studied by Gras et al. [8] in 2006. Alongside with these studies, the synthesis of $Mo(Si,Al)_2/SiC$, $MoSi_2/Al_2O_3$, $MoSi_2/WSi_2$ and, $MoSi_2/Mo_5Si_3$ were also studied [9–12]. But what is important is that during all the studies performed on the formation of $MoSi_2$ by SHS process in the presence of aluminum, this element was only taken into consideration as an enforcing agent constituent in $MoSi_2/Al_2O_3$ composite or as an intermetallic factor $Mo(Si_{1-x},Al_x)_2$. However, no attention has been paid to the role of this element during the SHS process so far. So, it has been tried in this research to perform X-ray diffraction (XRD), scanning electron microscope (SEM), differential thermal analysis (DTA), and on the other hand, the thermal profile to study the manner of aluminum affecting the process of the performance of $MoSi_2$ by SHS as a thermal source by employing microscopic studies.

## 2. Materials and experimental methods

All the specifications of raw materials such as molybdenum, silicon, and aluminum powders are presented in Table 1. Two sample groups were prepared to study the effect of the presence of aluminum on the process of SHS for the formation of $MoSi_2$. One group with stoichiometric mixture of Mo + 2Si (Mo: 33.3, Si: 66.7 in atomic percent) and another group with powder mixture of (Mo + 2Si) + 5 wt% Al named (MSA-0) and (MSA-5), respectively. The samples were compacted within a cylindrical steel frame under 180 kg/cm$^2$. After compacting the samples, the average diameter and height of the produced discs were 12.3 mm and 20 mm, respectively (Fig. 1). Also, oxy-acetylene flame was employed to provide the ignition temperature for the initiation of the reaction. The samples were first placed on a metal tripod and then were exposed to oxy-acetylene flame from the higher end. With the start of the reaction in the sample, the flame was turned off and due to the propagation of the combustion front in the sample, the reactive materials were transformed into products. According to Fig. 1, the thermal profile of the samples was obtained by a B-type thermocouple during the SHS. A data acquisition with a frequency of 100 kHz was employed for the collection of the thermocouple signals and their transfer to a computer.

In the next stage, the samples were studied for phase identification by XRD analysis (MPD-XPERT, Philips) and for microstructure by SEM (XL30 SERIES, Philips). The SEM was equipped with an energy dispersive spectrometer (EDS). The samples also

* Corresponding author. Tel.: +98 3113915739; fax: +98 3113912752.
*E-mail address:* panjepour@cc.iut.ac.ir (M. Panjepour).

0925-8388/$ – see front matter © 2010 Elsevier B.V. All rights reserved.
doi:10.1016/j.jallcom.2010.04.159

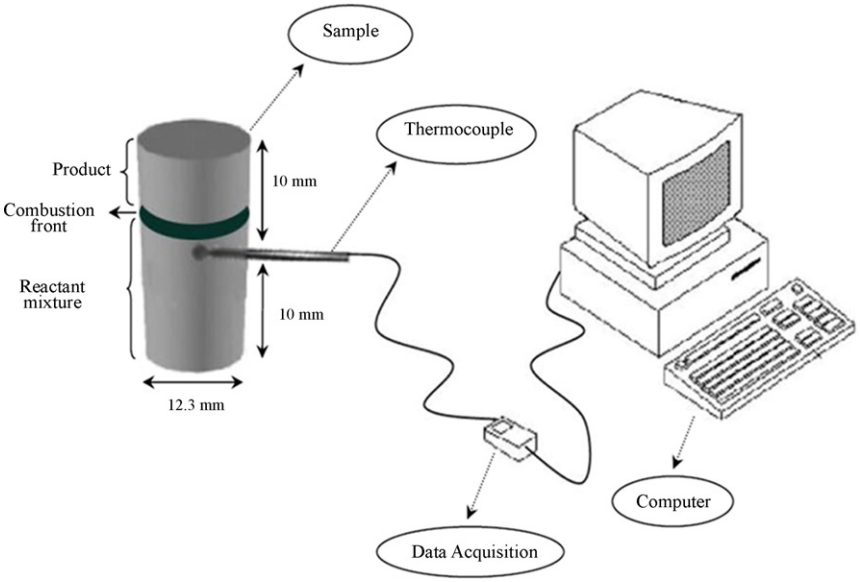


**Fig. 1.** Schematic representation of thermal profile for the samples obtained.

**Table 1**
The specifications of raw materials.

| Powder material | Particles size (μm) | Purity (%) | Company |
|---|---|---|---|
| Si | 1–10 | 99 | Merck |
| Mo | 1–40 | 99.9 | Merck |
| Al | 100–200 | 99 | Aldrich |

underwent differential thermal analysis (DTA) by the STA device (L70/2171, Linseis) to complete the results and to examine the effect of the presence of aluminum on the above SHS more precisely. The important parameters in this experiment such as heating rate, maximum heating temperature, and the weight of the samples were 20 °C/min, 1200 °C, and 36 mg, respectively.

## 3. Results and discussion

### 3.1. Thermal profiles

Fig. 2 depicts the recorded thermal profile during SHS reaction for the two samples of MSA-0 and MSA-5.

As it is observed in the figure, the maximum temperatures recorded by thermocouple for samples MSA-0 and MSA-5 are 1020 °C and 1400 °C, respectively. On the other hand, as it is observed, the maximum recorded temperature for the thermal profile of MSA-5 sample has been done in less time relative to MSA-0 sample. So, it can be inferred that the rate of the propagation of combustion front in MSA-5 sample is more than that in MSA-0 sample. It is also noticed that the rate of the sample cooling after the passage of the combustion front is less in MSA-5 relative to that of MSA-0. The smooth thermal gradient of the temperature profile diagram for MSA-5 sample relative to MSA-0 supports it pretty well. With regard to these facts, it can be inferred that the presence of aluminum effectively results in the increase of the maximum temperature at the combustion front (about 400 °C), the intense increase of the propagation rate of combustion front, and the decrease of cooling rate.

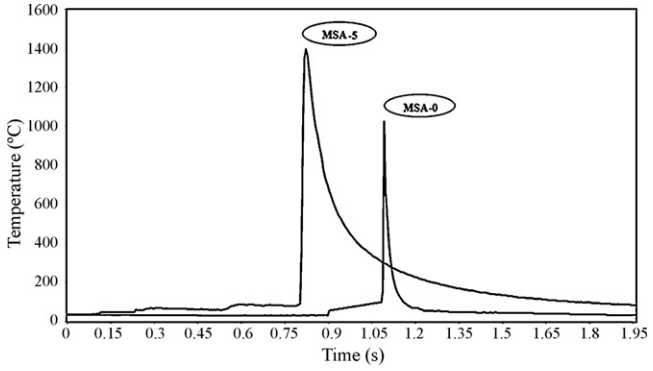


**Fig. 2.** The results of thermal profile for MSA-0 and MSA-5 during SHS reaction.

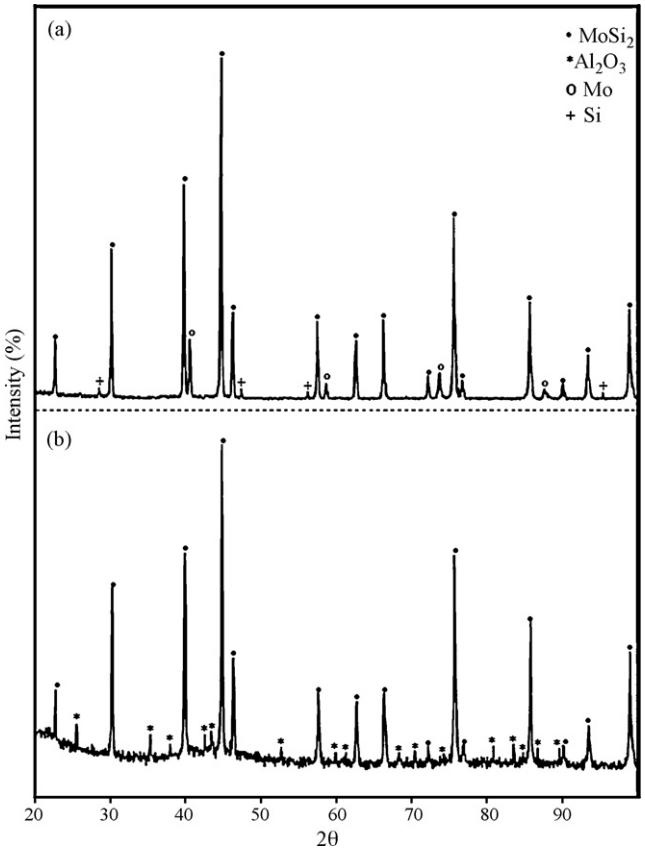


**Fig. 3.** XRD patterns after SHS synthesis for (a) MSA-0 and (b) MSA-5.

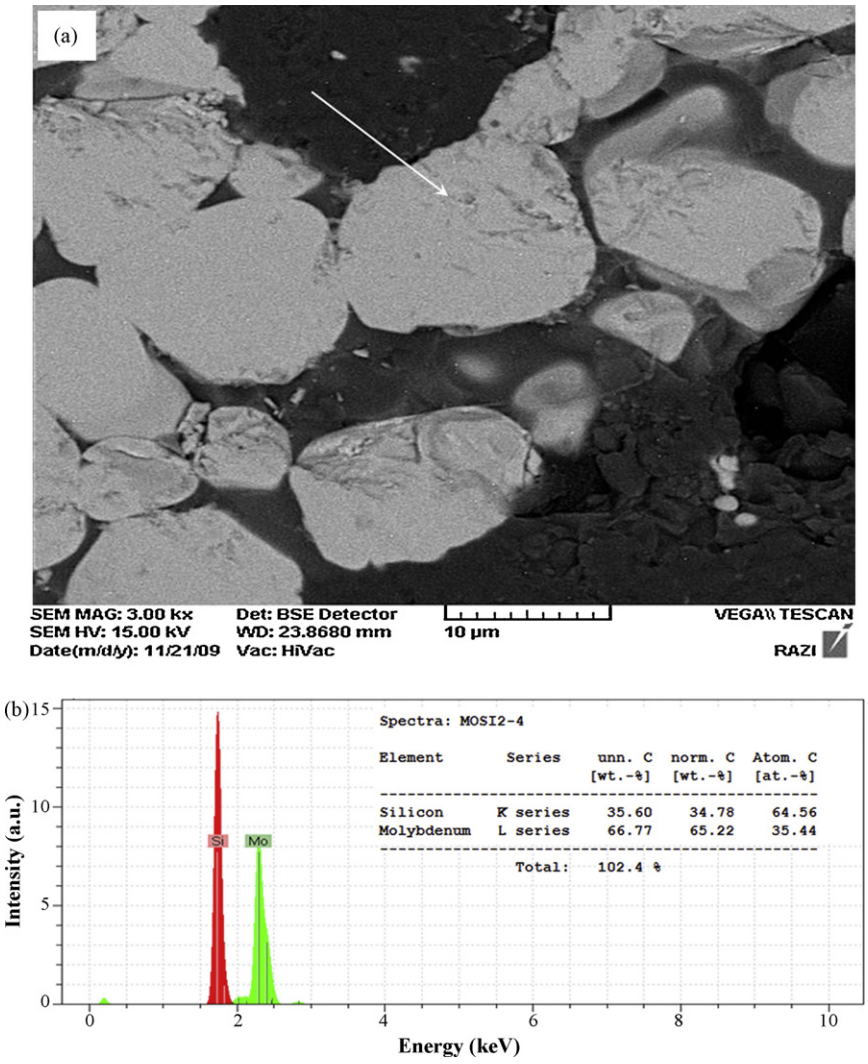


**Fig. 4.** (a) A SEM micrograph of MSA-0 after the SHS synthesis, (b) EDS pattern of the specified point.

### 3.2. Phase analysis

The products of the synthesized samples were analyzed through XRD to study the effect of the presence of aluminum on SHS process of $MoSi_2$ formation. The XRD patterns for the obtained products resulting from the synthesis of the two samples of MSA-0 and MSA-5 are depicted in Fig. 3. In Fig. 3a concerning the results obtained from the XRD pattern of the products related to MSA-0 sample, the $MoSi_2$ phase along with an amount of the remaining raw materials such as molybdenum and silicon are observed. While in Fig. 3b related to the result obtained from the XRD pattern of the products resulting from the MSA-5 sample, the $MoSi_2$ phase along with $Al_2O_3$ is observed and no trace of the unreacted raw materials is seen. This can be an indication of fact that in the presence of aluminum, the reaction takes place more completely and on the other hand, the aluminum present in the raw materials is entirely under the oxidation process and is oxidized into $Al_2O_3$ during the synthesizing process between the particles of molybdenum and silicon.

The important thing here is the lack of intermetallic phase of $Mo_5Si_3$ among the products. The cause of this phenomenon has been investigated by Seetharama [6]. He showed that at heating rates over 100 °C/min, only $MoSi_2$ phase is formed and it is only at heating rates lower than 100 °C/min that $Mo_5Si_3$ phase is formed. But as it is obvious from the recorded thermal profiles in Fig. 2, the heating rate is very higher than this value (100 °C/min), therefore it can be inferred that the obtained product through this SHS in real conditions is only the $MoSi_2$ phase. As it is observed, it is reasonably confirmed by XRD results (Fig. 3a and b).

### 3.3. Microstructural observations

Figs. 4a and 5a present the SEM micrographs of MSA-0 and MSA-5, respectively. While, the EDS analysis for the points specified on the SEM images are shown in Figs. 4b and 5b–d.

According to Fig. 4a and b, the equiaxed $MoSi_2$ grains can be deduced in the products of MSA-0 sample.

Fig. 5b–d is related to the EDS analysis for points 1, 2, and 3, respectively. The equiaxed $MoSi_2$ grains (Fig. 5b) along with $Al_2O_3$ particles (Fig. 5c) formed in the products of MSA-5 sample are fairly observed due to these results. Furthermore, some of the $MoSi_2$ particles imprisoned within the $Al_2O_3$ particles are fairly observed in Fig. 5d. The presence of $MoSi_2$ particles imprisoned within $Al_2O_3$ in a way proves the melting condition of $Al_2O_3$ particles when the combustion front is passing.

Therefore, according to these figures, it can be inferred that in the presence of aluminum, the temperature of the combustion front at least exceeds 2054 °C (melting point of $Al_2O_3$) in practical conditions. In fact, this temperature increase improves the conditions for the formation of $MoSi_2$ during the SHS.

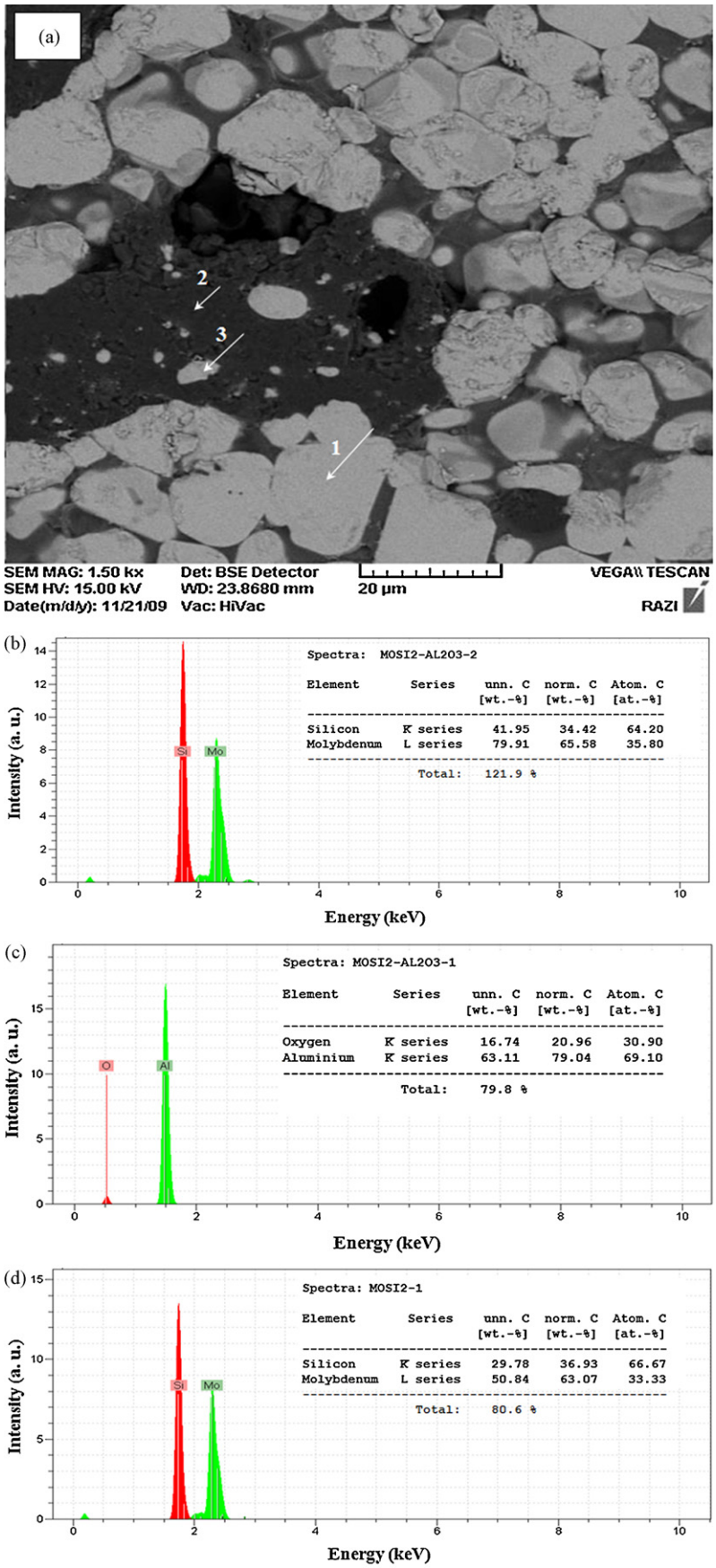


**Fig. 5.** (a) A SEM micrograph of MSA-5 after the SHS synthesis and EDS patterns of the specified points (b) 1, (c) 2 and (d) 3.

**Table 2**
Enthalpies of reactions for the formation of $MoSi_2$ in the presence of aluminum (air atmosphere).

| Reaction | $\Delta H_i$ | $\Delta H_i$ (kJ mol$^{-1}$) | Ref. |
|---|---|---|---|
| $[Mo_{(s)} + 2Si_{(s)} + 0.28Al_{(s)} + 0.21O_{2(g)}]_{298} \rightarrow [MoSi_{2(s)} + 0.14Al_2O_{3(s)}]_{298}$ | $\Delta H_1$ | −371.529 | [13,14] |
| $[MoSi_{2(s)} + 0.14Al_2O_{3(s)}]_{298} \rightarrow [MoSi_{2(s)} + 0.14Al_2O_{3(s)}]_{2293}$ | $\Delta H_2$ | 202.928 | [13] |
| $[MoSi_{2(s)} + 0.14Al_2O_{3(s)}]_{2293} \rightarrow [MoSi_{2(l)} + 0.14Al_2O_{3(s)}]_{2293}$ | $\Delta H_3$ | 85.001 | [15] |
| $[MoSi_{2(l)} + 0.14Al_2O_{3(s)}]_{2293} \rightarrow [MoSi_{2(l)} + 0.14Al_2O_{3(s)}]_{2327}$ | $\Delta H_4$ | 1.730 | [13] |
| $[MoSi_{2(l)} + 0.14Al_2O_{3(s)}]_{2327} \rightarrow [MoSi_{2(l)} + 0.14Al_2O_{3(l)}]_{2327}$ | $\Delta H_5$ | 15.551 | [13] |
| $[MoSi_{2(l)} + 0.14Al_2O_{3(l)}]_{2327} \rightarrow [MOSi_{2(l)} + 0.14Al_2O_{3(s)}]T_{ad}$ | $\Delta H_6$ | $\int_{2327}^{T_{ad}} [C_p^l(MoSi_2) + 0.14 * C_p^l(Al_2O_3)]dt$ | [13,16] |

### 3.4. Determination of adiabatic temperature

Theoretical computations can be used for the determination of adiabatic temperature in the presence of aluminum for an initial prediction and then with the help of thermal analysis studies, the manner of the effect of the presence of aluminum is also studied. Therefore, computation of the adiabatic temperature of the reaction in different conditions from the view of the presence of aluminum is studied in continuation.

First, it is important to note that aluminum can play two different roles depending on the type of the prevailing atmosphere as follows:

#### 3.4.1. Air atmosphere

If the reaction takes place in air atmosphere, the reaction in combustion front will take place in the manner of reaction (1). $\Delta H = 0$ is taken into consideration to obtain the adiabatic temperature in the reaction (Eq. (2)). It is required to mention that the amount of the existing aluminum by its weight percent was obtained to be equal to 0.28 mole for every mole of molybdenum. On the other hand, as it was observed in reaction (1), the amount of oxygen is only considered on the basis of aluminum oxidation reaction

$$Mo_{(s)} + 2Si_{(s)} + 0.28Al_{(s)} + 0.21O_{2(g)} \rightarrow MoSi_{2(l)} + 0.14Al_2O_{3(s)} \quad (1)$$

$$\Delta H = 0 \Rightarrow H_{reactants}|_{298} = H_{product}|_{T_{ad}} \quad (2)$$

Different stages of the reaction during these conditions and processes of the conversion of raw materials to products along with the required data for the enthalpy at each stage are presented in Table 2.

Under these conditions and with regard to the data presented in Table 2, the adiabatic temperature of the system was computed by Eqs. (2) and (3) to be 3462 K.

$$\Delta H = \Delta H_1 + \Delta H_2 + \Delta H_3 + \Delta H_4 + \Delta H_5 + \Delta H_6 = 0 \quad (3)$$

But, in the absence of aluminum, the SHS reaction takes place in accordance with reaction (4). Its different stages along with the required thermodynamic data for enthalpy of each stage are presented in Table 3.

$$Mo_{(s)} + 2Si_{(s)} \rightarrow MoSi_{2(s)} \quad (4)$$

With the help of thermodynamic data presented in Table 3 as well as with the help of Eq. (5), the existing adiabatic temperature in combustion front was equal to 2000.8 K in this state as well.

$$\Delta H = \Delta H_1 + \Delta H_2 = -136.9316 + \int_{298}^{T_{ad}} [C_p^s(MoSi_2)]dt = 0 \quad (5)$$

The obtained adiabatic temperature in this research is compared with the values of other references in Table 4. As it is observed, there is a good conformity between the results obtained from different references and this study.

Theoretical computations of adiabatic temperature show that if aluminum is present in the raw material mixture and oxygen is present in the prevailing atmosphere, this parameter is intensely increased in such a way that the combustion front temperature ($T_{ad}$ = 3462 K) is more than the melting temperature of $Al_2O_3$ (2352 K). A microscopic study performed by SEM (as Figs. 4 and 5) properly supports this theory.

#### 3.4.2. Oxygen-free atmosphere

If the reaction takes place in an oxygen-free atmosphere, aluminum particles do not enter the reaction and the reaction of SHS takes place as per reaction (6)

$$Mo_{(s)} + 2Si_{(s)} + 0.28Al_{(s)} \rightarrow MoSi_{2(l)} + 0.28Al_{(l)} \quad (6)$$

Different stages of the reaction and conversion of the raw materials to products along with data regarding the enthalpy at each stage are observed in Table 5.

With regard to the enthalpy values presented in Table 5 and with the help of Eq. (7), the temperature of adiabatic in this state is calculated at 1736 K.

$$\Delta H = \Delta H_1 + \Delta H_2 + \Delta H_3 + \Delta H_4 = 0 \quad (7)$$

**Table 3**
Enthalpies of reactions for the formation of $MoSi_2$.

| Reaction | $\Delta H_i$ | $\Delta H_i$ (kJ mol$^{-1}$) | Ref. |
|---|---|---|---|
| $[Mo_{(s)} + 2Si_{(s)}]_{298} \rightarrow [MoSi_{2(s)}]_{298}$ | $\Delta H_1$ | −136.932 | [14] |
| $[MoSi_{2(s)}]_{298} \rightarrow [MoSi_{2(s)}]_{T_{ad}}$ | $\Delta H_2$ | $\int_{298}^{T_{ad}} [C_p^s(MoSi_2)]dt$ | [13] |

**Table 4**
Compare the computed adiabatic temperature of the formation $MoSi_2$ by SHS in different references.

| Ref. | [8] | [17] and [18] | [19] | [20] | This work |
|---|---|---|---|---|---|
| $T_{ad}$ | ~1910 | ~2000 | ~1900 | ~1943 | 2000.8 |

**Table 5**
Enthalpies of reactions for the formation of $MoSi_2$ in the presence of aluminum (oxygen-free atmosphere).

| Reaction | $\Delta H_i$ | $\Delta H_i$ (kJ mol$^{-1}$) | Ref. |
|---|---|---|---|
| $[Mo_{(s)} + 2Si_{(s)} + 0.28Al_{(s)}]_{298} \rightarrow [MoSi_{2(s)} + 0.28Al_{(s)}]_{298}$ | $\Delta H_1$ | −136.932 | [14] |
| $[MoSi_{2(s)} + 0.28Al_{(s)}]_{298} \rightarrow [MoSi_{2(s)} + 0.28Al_{(l)}]_{933}$ | $\Delta H_2$ | 50.979 | [13] |
| $[MoSi_{2(s)} + 0.28Al_{(l)}]_{933} \rightarrow [MoSi_{2(s)} + 0.28Al_{(l)}]_{933}$ | $\Delta H_3$ | 10.711 | [13] |
| $[MoSi_{2(s)} + 0.28Al_{(l)}]_{933} \rightarrow [MoSi_2 + 0.28Al_{(l)}]T_{ad}$ | $\Delta H_4$ | $\int_{933}^{T_{ad}} [C_p^s(MoSi_2) + 0.28 * C_p^l(Al)dt]$ | [13] |

In this state, aluminum plays the role of a diluting agent, so that its presence only results in an adiabatic temperature drop. Therefore, according to Merzhanov standard, the above process cannot self-sufficiently progress under these conditions [21].

### 3.5. Differential thermal analysis (DTA)

Ultimately, to confirm the results obtained from the effect of aluminum on the trend of $MoSi_2$ formation during SHS, a powder mixture of the two samples of MSA-0 and MSA-5 went under DTA with the results depicted in Fig. 6.

As it is observed in Fig. 6a (DTA curve represents the MSA-0 sample), the curve is divided into three basic regions with the following reactions in these regions:

Region I: In this region an exothermic peak related to the solid–solid reaction is observed between molybdenum and silicon particles which are in contact with each other.
Region II: In this region an endothermic peak related to the melting of a part of silicon particles is observed.
Region III: An exothermic peak related to the dissolution of molybdenum particles in silicon melt and formation of $MoSi_2$ composition is also observed in this region.

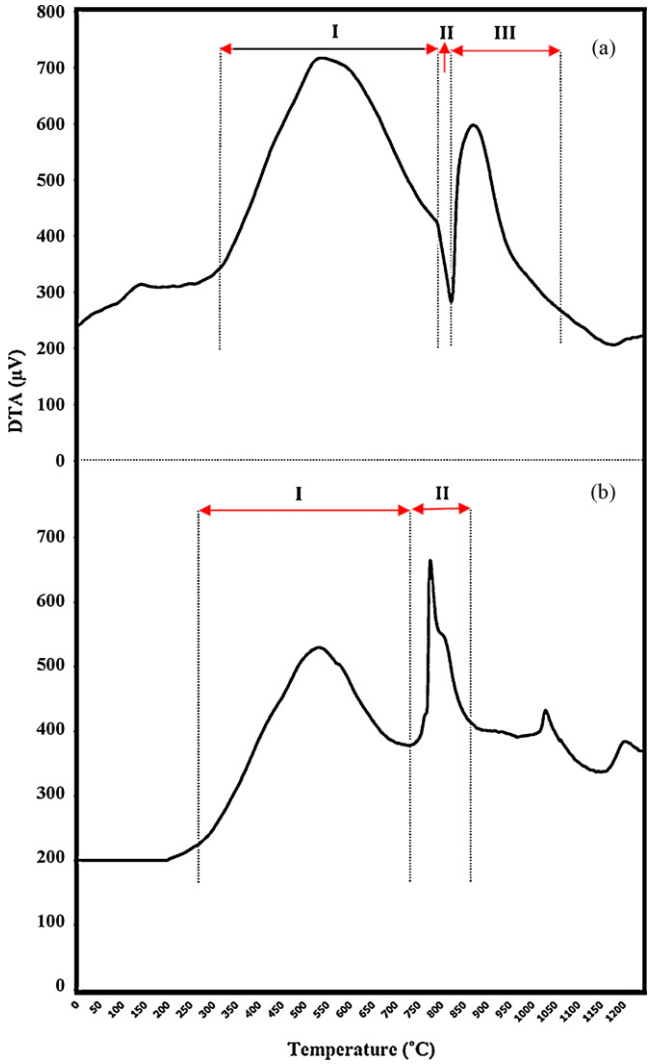


**Fig. 6.** Variations of DTA curve for (a) MSA-0 and (b) MSA-5.

Moreover, in Fig. 6b (DTA curve depicts the MSA-5 sample), the curve is divided into two basic regions:

Region I: In this region an exothermic peak related to the solid–solid reaction is observed between molybdenum and silicon particles which are in contact with each other and the oxidation of aluminum particles.
Region II: An exothermic peak related to the dissolution of molybdenum particles in silicon melt and formation of $MoSi_2$ composition is observed in this region (according to Seetharama studies [6]).

Thus, according to the curves in Fig. 6a and b, the diagrams obtained from the two samples have some differences which are pointed to as follows:

I. The DTA curve related to the MSA-0 sample includes three regions, while the DTA curve related to the MSA-5 consists of two regions. This is because of the deletion of the peak related to silicon melt in the presence of aluminum in Fig. 6b. In fact, it is the overlapping of the melt endothermic peak with the peak related to the oxidation of aluminum particles (exothermic reaction).
II. The region I in DTA curve for the MSA-5 (Fig. 6b) sample starts at lower temperatures (about 50 °C) relative to the MSA-0 sample (Fig. 6a). In fact, the cause of this phenomenon is the start of the oxidation of aluminum particles in this region followed by the sample temperature increase resulting in the improvement of the conditions for the start of penetrative reaction between molybdenum and silicon particles in solid state.
III. The peak related to the formation of $MoSi_2$ for the MSA-5 sample (the II region in Fig. 6b) has started at lower temperatures (about 80 °C) than the MSA-0 sample (the III region in Fig. 6a). This phenomenon is also due to aluminum oxidation reaction and the heat liberated from this reaction in the MSA-5 during SHS process. In other words, the liberated heat from this reaction creates conditions for the formation of $MoSi_2$ at lower temperature.

Therefore, as it was observed in these results, when the conditions for the oxidation reaction of aluminum particles in the MSA-5 sample are prepared, the heat resulting from this reaction can have a role as a thermal source in the combustion front. This results

in a temperature increase in the combustion front so that it can bring about appropriate conditions for better completion of the SHS reaction (according to Fig. 3). In other words, aluminum has varied effects on the formation trend of $MoSi_2$ during SHS process due to its oxidation reaction. For example, it can be referred to adiabatic temperature and movement rate in combustion front, reduction of the amount of the unreacted raw materials, and the starting time of the reactions which have been discussed in this study.

## 4. Conclusion

In this research the effect of the presence of aluminum on the powder mixture of Mo–Si raw materials during the formation of $MoSi_2$ by SHS process was studied. The research findings showed that the presence of aluminum particles in the mixture of raw materials can bring about the following cases by creating heat through aluminum oxidation reaction the formation of $MoSi_2$ by SHS process and formation of $Al_2O_3$:

- Intense changes will be observed in the thermal profile of the samples in the presence of aluminum. These changes are in a way that in the presence of aluminum, the increase of the speed rate of the movement of combustion front and reduction rate of cooling of the samples after combustion are observed by an intense increase of the maximum temperature.
- We will face a significant reduction in the raw materials in the products due to the liberation of the heat resulting from aluminum oxidation reaction during the formation of $MoSi_2$ by SHS process. In other words, the presence of aluminum in the mixture of raw materials and its oxidation results in an increase in the purity of the products.
- A part of the liberated heat resulted from aluminum oxidation will provide the heat required for melting of a part of silicon particles. Another part of this liberated heat increases the temperature of the sample resulting in the acceleration of the formation of $MoSi_2$ composition and this composition will form with shorter durations.

## References

[1] Y.L. Jeng, E.J. Lavernia, J. Mater. Sci. 29 (1994) 57–71.
[2] W.Y. Lin, L.Y. Hsu, R.F. Speyer, J. Am. Ceram. Soc. 77 (1994) 1162–1168.
[3] J.J. Petrovic, Intermetallics 8 (2000) 1175–1182.
[4] S.L. Kharatyan, A.R. Sarkisyan, Int. J. SHS 2 (1993) 323–332.
[5] Z. Yao, J. Stiglich, T.S. Sudarshan, J. Mater. Eng. Perform. 8 (1999) 291–304.
[6] C.D. Seetarama, Int. J. Refract. Mater. Sci. 39 (1995) 275–316.
[7] S.-W. Jo, G.-W. Lee, J.-T. Moon, Y.-S. Kim, Acta Mater. 44 (1996) 4317–4326.
[8] C. Gras, E. Gaffet, F. Bernard, Intermetallics 14 (2006) 521–529.
[9] C.L. Yeh, W.H. Chen, J. Alloy. Compd. 438 (2007) 165–170.
[10] J. Subrahmanyam, R. Mohan Rao, Mater. Sci. Eng. A183 (1994) 205–210.
[11] A.-L. Dumont, J.-P. Bonne, T. Chartier, J.M.F. Ferreira, J. Eur. Ceram. Soc. 21 (2001) 2353–2360.
[12] G.-J. Zhang, X.-M. Yue, T. Watanabe, J. Mater. Sci. 35 (2000) 4729–4733.
[13] I. Barin, Thermochemical Data of Pure Substances, third ed., Federal Republic of Germany, Weinheim, 1995.
[14] Y. Liu, G. Shao, P. Tsakiropoulos, Intermetallics 8 (2000) 953–962.
[15] X. Fan, T. Ishigaki, J. Cryst. Growth 171 (1997) 166–173.
[16] O. Kubaschewski, C.B. Alcock, Metallurgical Thermochemistry, vol. 24, fifth ed., International Series on Materials Science and Technology, 1979.
[17] Z.A. Munir, U. Anselmi-Tamburini, Mater. Sci. Rep. 3 (1989) 279–365.
[18] Z.A. Munir, Solid State Ionics 101–103 (1997) 991–1001.
[19] K. Ghosh, M.H. McCay, N.B. Dahotre, J. Mater. Process. Technol. 88 (1999) 169–179.
[20] J. Subrahamanyam, M. Vijayakumar, J. Mater. Sci. 27 (1992) 6237–6249.
[21] A.G. Merzhanov, J. Mater. Process. Technol. 56 (1996) 222–241.